Article

Geochemical implications of the weathering process of granitoids and formation of black soils - an example from the San'in district, Southwest Japan

Hiroaki Ishiga*, Kaori Dozen** and Chikako Yamazaki***

Abstract

Chemical weathering of granitoids and related sorting effect during formation of black soil have been evaluated in the Yokota area, San'in district, Southwest Japan. The Minari section examined consists of three zones (A, B, and C, in descending order) in terms of soil stratigraphy. The C zone consists of relatively fresh granitoids (C1), and weathered granitoids retaining original igneous structures (C2). The B zone consists of weathered granitoids (B1), including breccias in *masa* sand matrices; mineral grains are partly stained by iron oxide minerals (B2). The A zone consists of black soils which are rich in organic material, showing the highest LOI values (6-7 wt%) among the three zones. LOI and CIA gradually increase up-section, suggesting progressive weathering toward the ground surface, coupled with the effects of biochemical activity. SiO_2 contents show no great change in the C zone, but other major elements show weak decrease upward, excluding Fe_2O_3* and K_2O. On the A-CN-K diagram, some samples in the C and B zones show slight K-enrichment, and those of the A zone have highest CIA values. Additional black soil samples from the Yokota area continue the feldspar weathering trend toward the A apex, suggesting higher degrees of weathering than in the A zone at Minari, and/or sorting effect during formation of black soils.

Vertical profiles of Ni and Zn show little increase and Pb and Rb are more consistent. Zr, Hf, Th, Ce Nb and Ta show little change in this profile. Considering the mobility of these elements, Ti/Zr, Zr/Y and Th/Sc ratios are regarded as more representative of the source rock composition. REE patterns, Eu/Eu*, and La_N/Yb_N and Nd_N/Sm_N show the least variation in the stratigraphic column, reflecting the relative immobility of the REE during black soil pedogenesis.

Key words: geochemistry, soil, weathering, granitoids

Introduction

Black soils are widely distributed in the plains and mountain regions of the world; such soils are produced by active vegetation and/or macro and micro-bioactivity (Bowen, 1979; Abbot and Parker, 1981; Yamanoi, 1996). Soils are important components on the earth's surface (Fyfe, 1989), but comparatively few geochemical studies have been carried out on their bulk chemical composition, compared to studies of their organic matter (Bowen, 1979). Furthermore, reports on the stratigraphic variation of composition from parent rock to the soils are scarce. Feldspars are major constituents of the upper crust, and thus chemical weathering of feldspars is a significant process in soil formation (Nesbitt and Young, 1984; Fedo *et al.*, 1995). Many studies have examined on chemical weathering using bulk chemistry, especially the ratios between the immobile element Al and mobile Na, Ca and K (Nesbitt and Young, 1982; 1984, 1989; Fedo *et al.*, 1995, Nesbitt *et al.*, 1996). Sorting effects related to weathering is also an important factor controlling the geochemical composition of sediments (Nesbitt *et al.*, 1996). In general, finer grained sediments

tend to have more mafic composition than associated coarser grained sediments (Cullers *et al.*, 1988; Nesbitt and Young, 1989; and many others). The effect of sorting on chemical compositions has been examined in differing sedimentary environments such as glacial deposits (Nesbitt and Young, 1989), modern fluvial systems (Cullers *et al.*, 1978, 1988; Cullers, 1994) and turbidites (Roser and Korsch, 1986). The process of chemical weathering has been demonstrated by examination of intensely weathered sections from fresh parent rock through to laterite (Nesbitt and Markovics, 1997; Price *et al.*, 1991; Rainbird *et al.*, 1990). However, very few studies of soil formation and related chemical weathering have been made in the San'in district. Geochemical variation in the sequence from granitoid parent rocks to black soils can give a means of understanding element mobility and stability during the weathering process, and provide tests of the reliability of geochemical indices for evaluation of source rocks.

Geological background and sample collection

Regional geology

Cretaceous and Paleogene granitoids are widely distributed in the San'in district of Southwest Japan (Fig. 1). Locally these granitoids are known as the Daito granodiorite, which consists of medium- to coarse-grained hornblende-biotite granodiorite of the magnetite series (Ishihara, 1977). The Daito granodiorite was also intruded by fine- to medium

---

* Department of Geoscience, Shimane University, Matsue 690-8504, Japan
* Graduate of the M. Sc. of the Department of Geology, Shimane University in 1995.
*** Graduate of the M. Sc. of the Department of Geology, Shimane University in 1999.
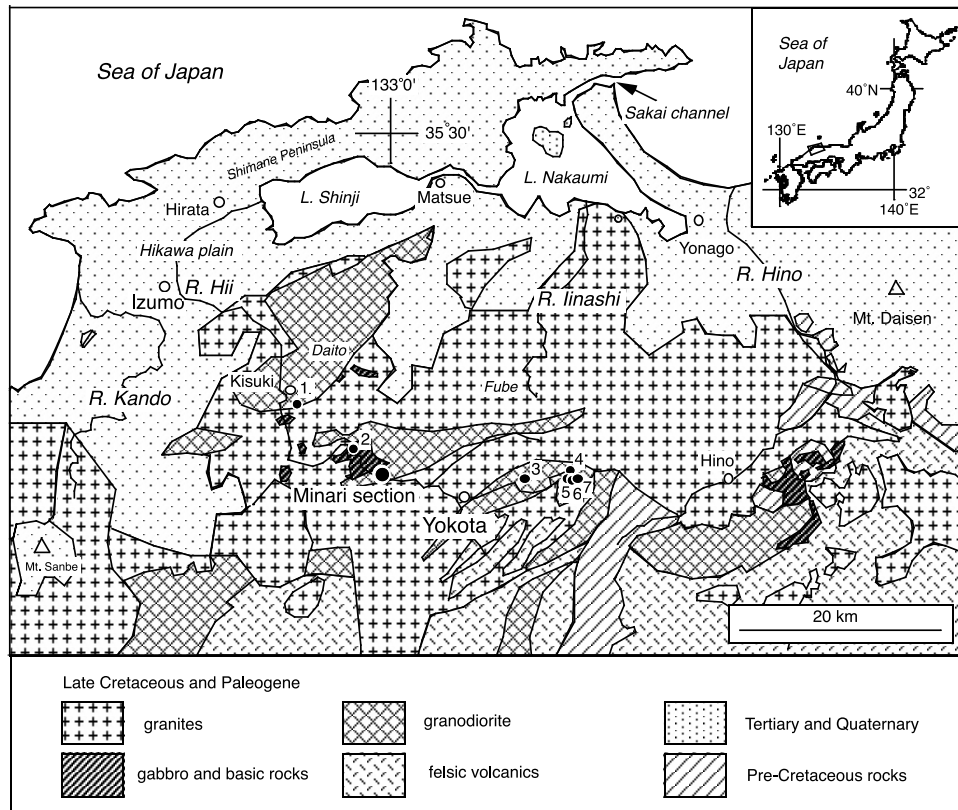
Fig. 1. Geological map of the central San'in district, Southwest Japan and location of the Minari section. Sample localities of additional black soils are also shown. Base map from Editorial Board of Geologic Map of Shimane Prefecture (1997).

grained biotite granite with transitional to sharp, irregular contacts (Kano *et al.*, 1994). K-Ar dating of the Daito granodiorites indicates an age range of 44-63 Ma (Kano *et al.*, 1994).

Magnetite sands derived from the San'in granitoids were utilized for high quality steel manufacturing, and thus sand processing had a great influence on both fluvial and coastal lagoon environments in the area (Tokuoka *et al.*, 1990). Sand processing in the mountains together with felling of forests for charcoal production extended the area stripped, and resulted in a deeply weathered wasteland which was readily eroded.

Tertiary sedimentary and volcanic complexes are distributed in sedimentary basins in the north of the district along the Japan Sea coast. Lower Miocene non-marine sediments unconformably overlie the basement granitoids, and thus Early Miocene paleoweathering may have been significant. The basins mainly developed along the Japan Sea coast during its opening, but small basins also occur sporadically in limited areas in the mountain regions (Fig. 1). However, no Tertiary sediments occur in our field area in the Yokota district.

Present climate of the San'in district

The vegetation of Southwest Japan belongs to the warm-temperate forest zone. Average temperature is 14°C,

with an annual range of 22-24°C. Total rainfall ranges from 1200 to 1500 mm per year, with heaviest falls in a rainy season in June and July.

Sample collection at Minari section

Samples were collected from an outcrop along highway Route 314, about 500 m northwest of Minari in Okuizumo town, Shimane Prefecture (Minari section in Fig. 1). Three gradational stratigraphic zones (A, B and C in descending order) were recognized within this section.

The lowermost C zone was subdivided into lower (C1) and the upper (C2) sub-zones based on the degree of weathering of the basement granitoids (columnar section in Fig. 2). The C1 sub-zone was composed of relatively fresh coarse-grained granodiorite containing hornblende and biotite. Fine-grained sericite flakes occurred within zoned plagioclase, suggesting slight alteration as a result of Quaternary weathering. Alteration is mostly concentrated along cleavages. The C2 sub-zone consisted of slightly weathered granodiorite, and was gradational between C1 and overlying B1 sub-zone. The texture of the rocks in the C2 sub-zone is identical to that of the underlying granodiorite, but their original mineralogy has been almost completely replaced. Plagioclase is almost completely altered to sericite, and quartz is slightly dissolved along subgrain boundaries, and at grain boundaries. Biotite is almost completely altered to

Table 1. XRF analyses of the parent rock (granodiorite), *masa* sands and black soils in the Minari section, and additional black soils from the Yokota area, San'in district of Southwest Japan. Numbers are sample numbers, in stratigraphically ascending order. Total Fe is given as Fe_2O_3*. CIA-Chemical Index of Alteration. Dash: not detected.

XRF sample	lithology	Oxides (wt. %) SiO_2	TiO_2	Al_2O_3	Fe_2O_3	MnO	MgO	CaO	Na_2O	K_2O	P_2O_5	Total	LOI	CIA	Trace elements (ppm) As	Ba	Ce	Cr	Cu	Nb	Ni	Pb	Rb	Sc	Sr	Th	V	Y	Zn	Zr
A zone																														
14	black soil	66.57	0.59	17.72	4.83	0.13	1.39	2.30	2.51	2.52	0.15	98.72	7.21	62	5	348	61	-	14	10	11	12	113	12	284	16	66	31	58	158
13	black soil	65.60	0.62	18.54	5.14	0.13	1.55	2.42	2.52	2.56	0.15	99.24	7.91	63	5	371	55	4	14	10	9	13	114	12	289	14	55	33	59	163
12	black soil	66.15	0.58	17.98	4.94	0.13	1.41	2.29	2.51	2.50	0.14	98.62	7.34	63	4	341	56	4	14	10	10	12	110	14	290	18	33	33	56	148
11	black soil	66.93	0.59	17.71	4.88	0.12	1.39	2.27	2.56	2.49	0.13	99.06	6.54	62	5	346	62	-	11	9	10	13	113	12	271	16	65	32	56	159
10	black soil	67.08	0.55	17.67	4.61	0.11	1.30	2.25	2.69	2.60	0.12	98.98	5.83	62	4	345	58	9	9	10	12	13	112	10	277	15	69	28	56	167
9	black soil	67.32	0.53	17.60	4.52	0.11	1.23	2.09	2.63	2.75	0.12	98.89	5.78	62	4	366	61	6	12	10	11	14	118	10	274	16	68	29	48	151
B zone																														
8	masa sand	67.65	0.57	17.47	4.63	0.11	1.30	2.14	2.62	2.63	0.12	99.23	5.46	62	4	379	56	-	7	10	9	14	117	8	269	15	72	28	56	178
7	masa sand	68.11	0.54	17.11	4.06	0.10	1.24	2.11	2.61	2.58	0.11	98.58	5.52	62	4	355	50	2	12	9	11	13	112	12	273	15	60	30	53	160
6	masa sand	72.26	0.42	14.85	1.83	0.06	0.94	2.01	2.90	3.09	0.06	98.43	2.67	56	3	445	41	-	11	10	10	13	116	8	272	10	72	22	38	164
5	masa sand	73.07	0.46	14.61	2.08	0.06	1.01	2.10	2.80	2.78	0.08	99.04	3.15	57	3	429	40	-	9	11	4	11	105	8	273	19	49	26	37	152
C zone																														
4	weathered Gd	72.32	0.28	14.06	3.12	0.05	0.51	1.60	3.25	3.48	0.07	98.74	1.29	54	3	450	40	-	5	8	7	9	114	6	234	16	22	18	28	100
3	weathered Gd	70.40	0.33	14.39	3.43	0.07	0.67	2.10	3.45	3.00	0.09	97.92	0.91	53	3	270	46	2	11	9	7	9	108	7	257	17	38	25	29	111
2	Granodiorite	71.49	0.40	14.39	2.65	0.07	0.89	2.73	3.68	2.39	0.10	98.79	0.40	52	2	378	58	-	6	10	8	10	95	6	311	15	30	22	34	147
1	Granodiorite	69.98	0.35	15.22	2.65	0.07	0.77	2.67	3.75	2.85	0.11	98.41	0.66	52	3	479	52	-	5	9	7	14	99	7	347	13	21	21	34	122
Additional black soils																														
sample no.																														
1		66.73	0.64	18.29	4.77	0.09	1.92	2.30	2.35	2.65	0.15	99.88	7.30	63																
2		65.06	0.72	19.68	6.01	0.13	1.86	2.22	1.86	2.15	0.09	99.76	10.74	68																
3		71.81	0.51	16.05	4.08	0.08	0.91	1.35	1.73	2.99	0.10	99.60	6.89	66																
4		69.50	0.48	16.38	3.93	0.10	1.10	2.11	2.87	2.67	0.12	99.25	5.15	59																
5		68.20	0.55	17.77	4.67	0.16	1.14	1.89	2.29	2.29	0.16	99.10	11.45	66																
6		66.43	0.67	18.35	5.58	0.15	1.25	1.50	2.25	2.69	0.15	98.99	9.56	67																
7		65.69	0.70	18.58	6.09	0.13	1.42	1.56	2.20	2.83	0.11	99.29	6.13	67																

chlorite, and biotite pseudomorphs can be recognized by patchy concentrations of fine-grained chlorite, muscovite, apatite, zircon, and iron oxides. The C2 sub-zone ranges up to about 3 m in thickness, and grades upward into the overlying B1 sub-zone.

The B zone is composed of breccias, and is subdivided into lower (B1) and upper (B2) sub-zones granitoids (columnar section in Fig. 2), based on grain size and mode of alteration. The B1 sub-zone consists of angular clasts set in a sandy matrix (*masa* sand). Clasts range from 1 to 2 cm in diameter, and consist solely of granodiorite as seen in the C zone. The sandy matrix is reddish brown (5YR 4/8-5YR3/6, standard soil color chart), and is rich in iron oxide minerals. The B1 sub-zone ranges up to 1.3 m in thickness. Grain size of the clasts decreases gradually upward into the B2 sub-zone. The B2 sub-zone contains finer grained detritus relative to the B1 sub-zone, but also contains clasts of granodiorite. The hues in this zone are darker than those of the B1 sub-zone, ranging from 5YR 4/4 to 5YR 3/3. The B2 sub-zone ranges up to 1.8 m in thickness, and grades into the A zone of black soils.

The A zone is composed of olive black to black soils (7.5Y 3/1-7.5Y 2/1) reaching 3.1 m in thickness granitoids (columnar section in Fig. 2). This soil develops crumb and granular structures, and is rich in humus. Plant roots also occur in this zone.

Additional soil samples from the Yokota area

Black soils are widely distributed in the Yokota area. Supplementary soil samples were collected in this area along the Hii River (Fig. 1) for comparison of composition with the Minari section, and for further evaluation of the weathering process and the degree of weathering.

Samples were collected at Kisuki (no. 1 in Fig. 1), near the Minari section (no. 2), and in the northeastern part of Yokota town (nos. 3- 7), where black soils several tens of cm in thickness are developed. Parent rocks at all sites were granodiorite similar in composition to that at the Minari section.

Gradual change from granodiorite parent rock through *masa* sand to black soil is similar to the change observed in the Minari section. The supplementary soils were all brownish black (YR 2 00), and were composed of soft round materials ranging from 1 to 5 mm in diameter. Loss on ignition (LOI) values ranged from 5 to 10 wt%, indicating higher concentrations of organic matter compared to those of the A zone in the Minari section (LOI < 7.9 wt%, Table 1).

Analytical methods

This study includes major, trace and REE (rare earth element) analyses of the samples from the three zones at Minari section, and major element analyses of the black soils collected from the Yokota area.

1. X-ray fluorescence (XRF) determinations of major element (SiO_2, TiO_2, Al_2O_3, Fe_2O_3*, MnO, MgO, CaO, Na_2O, K_2O, and P_2O_5) and trace element (V, Cr, Ni, Cu, Zn, Y, Zr, Nb, Rb, Sr, and Ba) abundances were made using a RIX-2000 XRF system (Rigaku Denki Co. Ltd.) at Shimane University. Total iron is expressed as Fe_2O_3*. Analyses of these elements were made on glass beads prepared with lithium tetraborate flux, with a flux to sample ratio of 5:1, basically following the method of Norrish and Hutton (1969). Additional trace elements (Th, Ce, Sc, Pb and As) were analyzed by glass bead method using a mixed lithium tetraborate-lithium metaborate flux (ratio of 4:1, respectively) with flux to sample ratio of 2:1, following the method of Kimura and Yamada (1996). Analytical errors for USGS standard rock SCo-1 (Cody Shale) were within ± 10% of recommended values for all trace elements except Cu, V, and Y.

2. Instrumental Neutron Activation Analysis (INAA) was used to determine the abundance of rare earth elements (La, Ce, Nd, Sm, Eu, Tb, Yb and Lu), and Cs, Hf and Ta in six selected samples from the Minari section. The analysis was carried out in the Research Reactor Institute of Kyoto University. Sample preparation, analytical methods and

precision are described by Musashino (1990). Average errors for these elements are less than ±10%, and results for SCo-1 were acceptable compared to values given in Potts *et al.* (1992).

Although Ce results show differences between the two analytical methods (XRF and INAA), ranging from 0.4% to 25%, this difference is not significant for the purposes of the discussion. The XRF Ce results were used for the vertical profiles, to retain relativity with other elements analyzed by this method, whereas the INAA Ce data were used for the chondrite-normalized REE patterns. The Eu anomaly (Eu/Eu*) was calculated using the formula:

$$Eu/Eu* = Eu_N/(Sm_N \times Gd_N)^{1/2} \text{ (Condie, 1993)};$$

where $Gd = (Sm \times Tb^2)^{1/3}$, and N=chondrite-normalized values (Taylor and McLennan, 1985).

Results are given in Tables 1 and 2, with data expressed on an ignited basis (after determination of LOI). Loss on ignition was determined by ignition of powdered samples at 1050°C in a muffle furnace for 1 hour.

Stratigraphic variation in composition, Minari section

Loss on Ignition

In general, loss on ignition is significantly correlated with contents of H_2O, total organic carbon (TOC), carbonate carbon (CC) and total sulfur (TS included in sulfate and sulfide material). In acid soils in Japan, soil formation is rarely related to sulfur and carbonate carbon concentrations (Yamanoi, 1996), and LOI is thus useful for evaluation of variation of organic matter in such soils. Carbonate mineral precipitation is limited during formation of organic matter rich soils, since they form under lower pH conditions resulting from decomposition of organic matter (HCOOH and other acids). Furthermore, carbonate rocks and sulfur mineralization do not occur in the Yokota area.

LOI values (Table 1) show gradual increase from the granodiorite in the C1 sub-zone (<0.7 wt%) toward the A zone (>7 wt%), suggesting up-section concentration of organic matter related to soil formation.

Enrichment factors

To examine gains or losses of each element in the stratigraphic column, the concentrations of each element were normalized against the composition of the granodiorite parent rock. Sample no. 1 is regarded as representative, and is very similar to the source of the weathered products, even though it has a Chemical Index of Alteration (CIA; Nesbitt and Young, 1982) ratio slightly greater than 50 (CIA=52), showing very slightly affected by chemical weathering. The normalized values are also indexed against the concentrations of Al_2O_3, because this oxide is relatively immobile during weathering, as is TiO_2 (Rainbird *et al.*, 1990; Nesbitt and Markovics, 1997).

The formula indicating enrichment or depletion related to weathering from the source rock is:

Enrichment of element X $(E_x) = (\text{Sample } Cx/CAl_2O_3)/(\text{granodiorite } Cx/CAl_2O_3)$,

where Cx is concentration of element X. Stratigraphic variations of Ex are illustrated in Figs. 2, 3 and 4.

Major elements

Silica is slightly enriched in the C-zone and the B1 sub-zone relative to the parent rock (E_x=up to 1.1) before decreasing sharply in the B2 to A zones, with levels less than 0.85x compared to the parent (Fig. 2). TiO_2, Fe_2O_3* and MgO show enrichment in the B2 and A zones relative to the C zone and the B1 sub-zone. Fe_2O_3* shows the greatest depletion in the B1 sub-zone, with E_x values as low as 0.8 (Fig. 2).

Enrichment factors for alkali and alkaline earth elements excluding MgO show gradual depletion up-section, suggesting leaching related to progressive weathering (Wronkiewicz and Condie, 1987; Nesbitt and Young, 1989; Fedo *et al.*, 1995). Among these elements Na_2O show the strongest depletion, with E_x falling from values near the parent (E_x ~1) in the C2 zone to depletion of <0.6 in the A zone. K_2O is slightly enriched in C2 and B1, but then steadily decreases to E_x ~0.8 in the zone A; CaO shows relatively uniform depletion from C2 through to A, also with E_x ~0.8 (Fig. 2). In contrast, P_2O_5 shows depletion in the C2 and B1 sub-zones, before becoming progressively enriched up-section (Fig. 2).
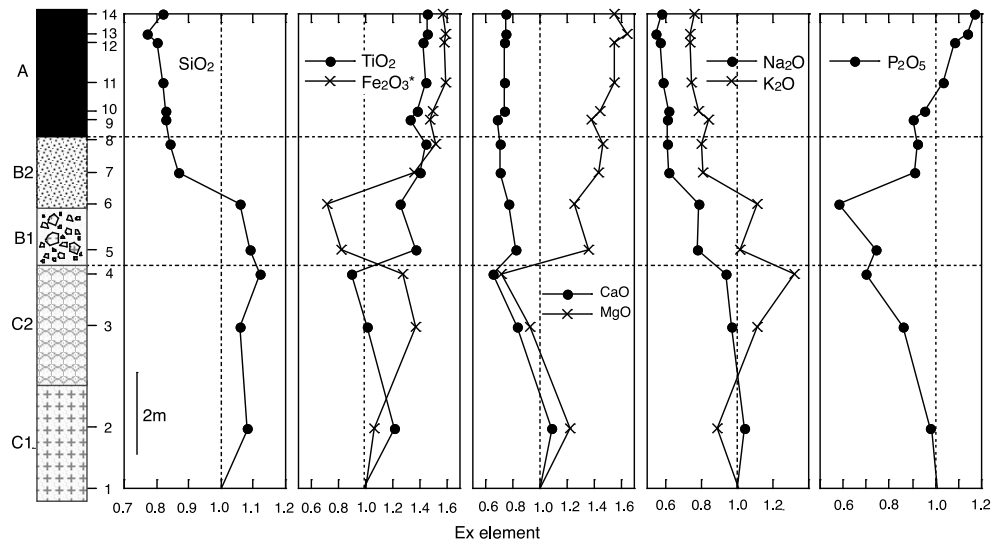
Trace elements

Stratigraphic variation of enrichment factors for trace elements in this section is rather more varied than those of the major elements, and vertical variations are not consistent. Vanadium and Cu show depletion in the upper part of the C2 sub-zone, and are characterized by enrichment in the B1 and the top of the A1 sub-zones, with variation in other zones (Fig. 3). Nickel and Zn show relatively consistent behaviour, with parent-like contents in the zone C, steady increase in the zone B, and quite uniform enrichment in the zone A, with E_x of ~1.2 and 1.5 respectively. Lead generally shows depletion relative to parent rock throughout the section, and a pattern that is almost a mirror image of the arsenic variation. Arsenic shows gradual increase up-section with some variation (Fig. 3). This variation, however, may be related to change in Al_2O_3 concentration, because the total range in As content (3 to 5 ppm) in the section is limited compared with that of Al_2O_3.

Rubidium shows small enrichments in the upper part of the C2 and B1 sub-zones, possibly related to K-metasomatism, as described later in the A-CN-K diagram. Cesium shows a gradual increase up-section. Strontium and Ba also show some relative enrichment in the same samples (Fig. 3), suggesting tendency for adsorption on clay minerals or residence in feldspar in association with Na_2O, CaO and K_2O (Wronkiewicz and Condie, 1987; Nesbitt and Young, 1989). Strontium and Ba, however, show consistent depletion (x 0.6) in the A zone, probably related to progressive weathering.

Yttrium, Zr, Th, Sc and REE are relatively less mobile during weathering processes, and generally show abundances similar to the source material (Taylor and McLennan, 1985; Condie, 1993; Roser *et al.*, 1996). Yttrium shows gradual enrichment to 1.3x of the levels in the parent rock, although with considerable variation (Fig. 4). Zirconium shows most enrichment in the B1 sub-zone, which is richest in coarser clastics (Fig. 4). This enrichment is probably related to heavy mineral concentration, such as zircon and/or monazite (Taylor and McLennan, 1985) in the B1 sub-zone. Zirconium contents then gradually decrease toward the top of the section. This is possibly related to decrease in grain size of the weathered materials, and related mineral sorting

in the A zone (Fig. 4). Thorium also shows enrichment toward the B1 sub-zone, but in the B2 and the A zones is present at levels comparable to those in the parent rock. In contrast, Ce shows depletion in the C2 to B2 sub-zones, and returns to parent rock levels in the lower part of the A zone. Scandium gradually increases toward the A zone, with some irregularity, and shows a pattern similar to the change in TiO_2 (Figs. 2 and 4).

Niobium and Ta show little systematic variation in enrichment factors, with all values lying in the range E_x 0.9-1.3 (Fig. 4). Total REE contents ($\sum$REE) in the section range from 95 to 126 ppm (Table 2). Vertical change of REE patterns and other indices are discussed later in this paper.
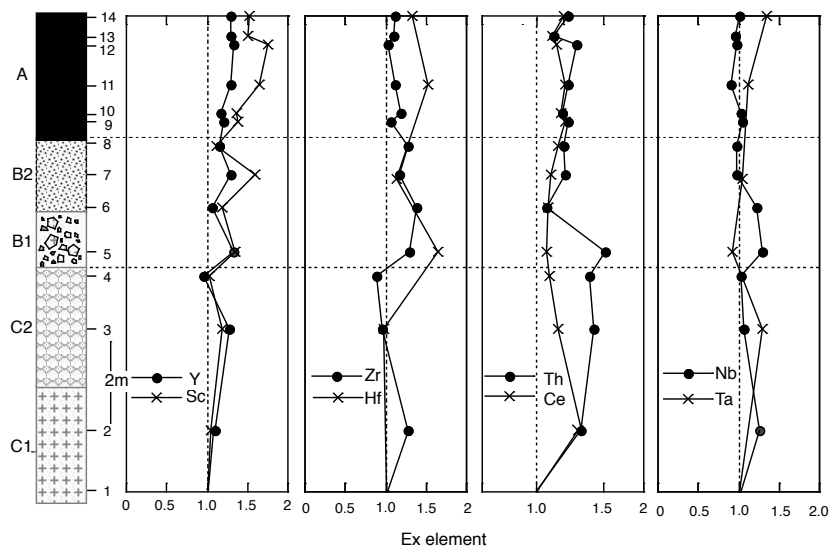

Fig. 2. Stratigraphic variation of major element enrichment factors (Ex element, see text) in the Minari section, San'in district of Southwest Japan.
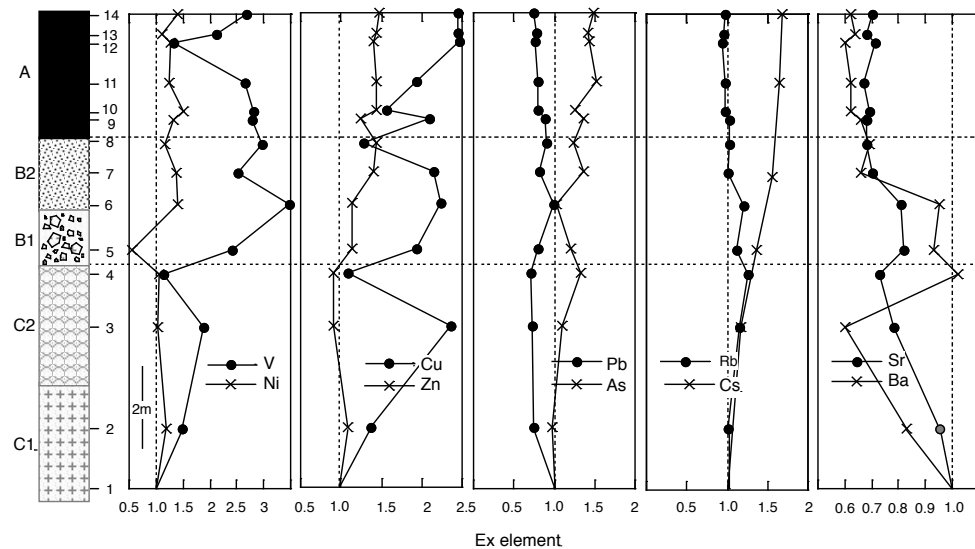
Fig. 3. Stratigraphic variation of trace element enrichment factors (Ex element, see text) in the Minari section, San'in district of Southwest Japan.

Table 2. INAA analyses of six selected samples from the Minari section, San'in district, Southwest Japan. Eu anomaly (Eu/Eu*) is calculated by the formula (Condie, 1993): $Eu/Eu^* = Eu_N/(Sm_N \times Gd_N)^{1/2}$, where $Gd = (Sm \times Tb^2)^{1/3}$. N = chondrite-normalized values (Taylor and McLennan, 1985).

INAA		(ppm) La	Ce	Nd	Sm	Eu	Tb	Yb	Lu	ΣREE	Cs	Hf	Ta	La$_N$/Yb$_N$	Nd$_N$/Sm$_N$	Eu/Eu*
A zone																
14	black soil	28.9	51.8	25.8	4.6	0.9	0.5	2.3	0.5	115.2	4.2	4.5	0.9	8.46	1.81	0.66
11	black soil	30.1	57.9	27.5	5.3	0.8	0.8	2.8	0.5	125.7	4.1	5.2	0.8	7.26	1.70	0.51
B zone																
7	*masa* sand	26.1	50.3	21.4	4.4	0.8	0.6	2.3	0.4	106.3	3.9	3.9	0.7	7.60	1.59	0.60
5	*masa* sand	17.6	53.0	17.0	3.8	0.7	0.5	2.0	0.4	95.0	3.4	5.6	0.6	6.02	1.45	0.59
C zone																
3	weathered Gd	26.5	53.2	24.4	4.4	0.7	0.6	2.5	0.4	112.7	2.9	3.3	0.9	7.22	1.81	0.49
1	Granodiorite	21.7	51.7	22.8	3.4	0.7	0.5	1.9	0.4	103.0	2.5	3.4	0.7	7.68	2.17	0.62

Fig. 4. Stratigraphic variation of trace element enrichment factors (Ex element, see text) in the Minari section, San'in district of Southwest Japan.

Weathering process

The Chemical Index of Alteration (CIA) of Nesbitt and Young (1982, 1984) was used to evaluate the degree of weathering. CIA is defined as:

$$CIA = [Al_2O_3/(Al_2O_3 + Na_2O + CaO^* + K_2O)] \times 100;$$

calculated as molar proportions, where CaO* represents the CaO present in silicate minerals only (Nesbitt *et al.*, 1982). The slightly elevated CIA of the parent rock (CIA = 52 for sample 1 of the C1 zone) relative to average granodiorite reflects very weak alteration due to chemical weathering. This is probably related to the alteration of plagioclase observed in thin section. Fine-grained mica flakes occurs in the cores of plagioclase crystals. This mineral formation suggests that alteration proceeded in relatively Ca-rich part of the plagioclases. CIA values in the C1 and C2 sub-zones show gradual increase upward (CIA = 54), suggesting that progressive weathering has occurred.

The CIA values clearly demonstrate that rocks examined in the section show gradual increase toward the A zone (Table 1). The values, however, show an abrupt change between the B1 sub-zone (around 56) and the B2 sub-zone (over 60), suggesting sorting effect for finer detritus in the B2 zone and in the soils of the A zone (Nesbitt *et al.*, 1996). The highest values (63-68) are found in the supplementary soils from the Yokota district (Table 1). Nevertheless, the CIA values overall are still lower than those of the Tertiary sedimentary rocks in the San'in district (CIA = 70 to 7; Ishiga and Dozen, 1997). This suggests that even the Yokota soils were affected by relatively lower degrees of weathering compared to those of the Tertiary environment.

A-CN-K and A-CNK-FM diagrams

These diagrams are useful for evaluation of chemical weathering of rocks and their degrees and processes (Nesbitt *et al.*, 1989; Fedo *et al.*, 1995). Sorting effects produced during the formation of finer particles or clays related to weathering can be displayed on the diagrams (Nesbitt *et al.*,

1996; 1997). The lowest sample of the fresh parent rock has composition similar to average granodiorite (Gd). One rock sample from the C1 sub-zone and two weathered rocks from the C2 sub-zone show slight displacement oblique to the A-CN edge (Fig. 5). This shows K_2O enrichment, possibly due to K-metasomatism (Fedo *et al.*, 1995), or to slightly higher K-feldspar contents in these samples. Samples of *masa* sand from the B1 and B2 sub-zones and black soils from the A zone trend away from the C2 sub-zone toward the A apex, suggesting enrichment in Al_2O_3 and depletion in CaO and Na_2O due to progressive destruction of plagioclase. Seven black soils from the Yokota area plot at higher positions than from the Minari section but on the same trend, suggesting more significant chemical alteration and/or sorting related to production of finer material (Nesbitt *et al.*, 1996, 1997). The data collectively run parallel to the A-CN edge, and thus form an ideal weathering trend typical of *in situ* alteration of crystalline rocks (Nesbitt and Young, 1984).

The A-CNK-FM diagram (Nesbitt and Young, 1984) also shows the process of weathering of granodiorite. Values for the relatively fresh rocks from the C1 sub-zone plot near the compositional trend connecting the FM apex and feldspar (FEL) composition), while *masa* sands, A zone samples, and the Yokota soils plot apart from the parent composition, forming a trend towards smectite (Sm) and the CNK-FM join (indicated by an arched arrow). This pattern is also evident in stream sediments for the Hino River (Ortiz and Roser, 2006), and suggests smectite is a significant alteration phase (Fig. 5).

Discussion

Soil formation and compositional changes

Soil is a product of weathered parent rocks which are mixed with organic matter by biogenic activity and bacterial biomineralization (Bowen, 1979 etc.). As shown by the CIA values and the A-CN-K diagram for the samples from the Minari section, chemical weathering partially leached Na_2O, CaO and K_2O during the transformation of feldspar to clays (Nesbitt and Young, 1984; 1989). Silica dissolution is demonstrated for the finer *masa* sand of the B2 sub-zone and black soils of the A zone. The black soils show 0.8x depletion in SiO_2 compared to the parent rocks (Fig. 2). Enrichment factors for Al_2O_3, TiO_2, Fe_2O_3*, MgO and P_2O_5 range from 1.1 to 1.4x, due to the loss of silica and the alkali and alkaline earth elements mentioned above. Vanadium and Cu concentrations of the A zone show enrichment compared to those of the parent rock. Increase in transition elements in accordance with the CIA values has been reported from weathering profiles of granodiorite (Nesbitt and Markovics, 1997). Al_2O_3 enrichment related to sorting effect (Nesbitt *et al.*, 1997) is indicated in the A-CN-K diagram (Fig. 5), where the weathering trend parallels the A-CN join, trending towards the A-apex. Sorting effect on the composition of the black soil in the Minari
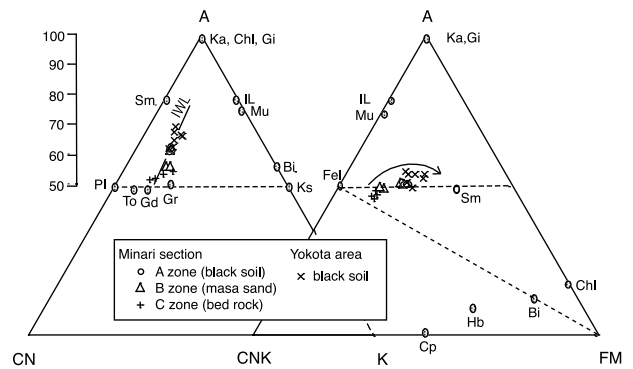
Fig. 5. A-CN-K and A-CNK-FM diagrams (after Nesbitt and Young, 1984; Fedo *et al.*, 1995) and CIA (Chemical Index of Alteration) from parent rocks (granodiorite) to black soils in the Minari section, San'in district of Southwest Japan. Additional black soil samples from the Yokota area are also plotted. Average compositions of granites (Gr), granodiorite (Gd) and tonalite (To) are also given for estimation of source compositions, after Condie (1993). Abbreviations: Ka, kaolinite; Chl, chlorite; Gi, gibbsite; Sm, smectite; IL, illite; Mu, Muscovite; Bi, Biotite; Pl, plagioclase; Ks, K-feldspar; Cp, clinopyroxene; Hb, hornblende; Fel, feldspar. IWL is an ideal weathering trend (Nesbitt and Young, 1984), later called the predicted ideal feldspar weathering trend (Roser and Korsch, 1999).

section is indicated by SiO_2/TiO_2 ratios (Fig. 6). Ratios in the C zone range from 180 to 254, whereas those in the A zone range from only 106 to 126. TiO_2 concentrations correlate well with those of Al_2O_3 in the section, showing finer material was formed during the weathering process. Zirconium depletion up-section from the *masa* sand of the B2 sub-zone to the black soils in the A zone is related to such sorting effect and mineral concentration. This may be due to zircon concentration in silt-sized sediments or fine sand (Taylor and McLennan, 1985), compared to the relatively finer grained soils of the A zone. The 5 m thick column from the *masa* sand to the black soils can thus represent a sedimentary sequence, where physical pumping of finer minerals up-section is significant in determining the composition of the black soils.

Zr/Y ratios show similar variation to those of Ti/Zr ratios in the vertical section, for Y may be concentrated in apatite, which behaves similarly to fine-grained minerals during sedimentary processes (Taylor and McLennan, 1985). Consequently, Ti/Zr and Zr/Y ratios show smaller variations compared to SiO_2/TiO_2 ratios.

Geochemical indices for provenance

Various indices have been proposed as provenance signatures, but among these Th/Sc ratios and REE parameters are most utilized, due to for their stability during sedimentary processes (Taylor and McLennan, 1985; Condie, 1993; McLennan *et al.*, 1993). Such geochemical indices are tested in the weathering profile of the Minari section.
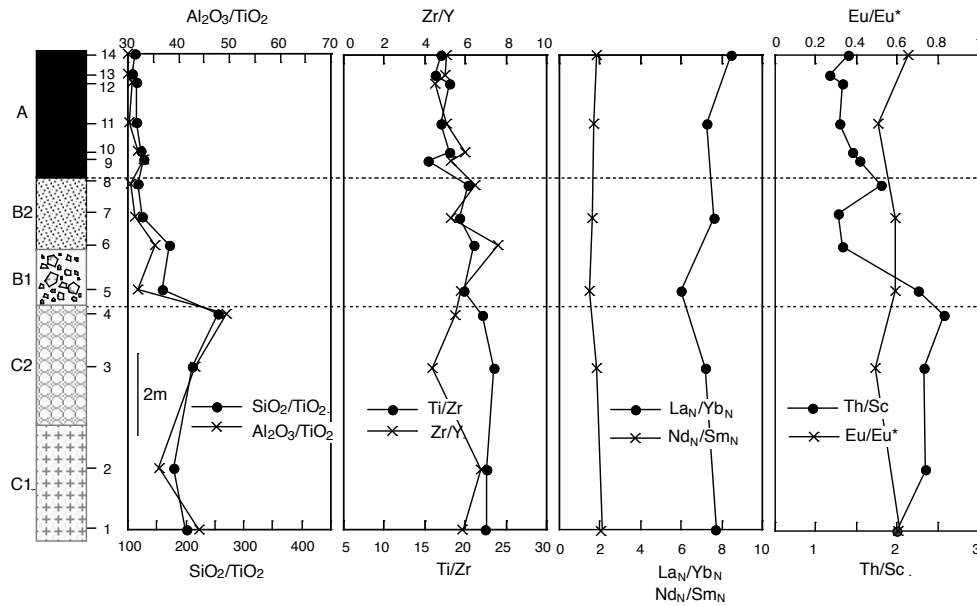
Fig. 6. Stratigraphic variation of elemental ratios and chondrite-normalized REE ratios from parent rock (granodiorite) to black soils in the Minari section, San'in district of Southwest Japan.

Th/Sc ratios

Thorium and Sc show most contrast in their distribution from felsic to basic rocks, as a result of igneous processes. Th/Sc ratios are thus often utilized for evaluation of provenance (Taylor and McLennan, 1985; Condie, 1993; Roser *et al.*, 1995). The Th/Sc ratio changes by a factor of about two times in the present section, ranging from 1.2 to 2.6 (Fig. 6). Variations by a factor of two are insignificant when provenances are evaluated by this index (Nesbitt and Markovics, 1997). Th/Sc ratios, however, vary by more than a hundred-fold in major rock types (Condie, 1993), and in sedimentary rocks derived from different sources (McLennan *et al.*, 1993). Th/Sc ratios therefore provide reliable provenance signatures (Nesbitt and Markovics, 1997).

In the Minari section, Th shows enrichment from the C zone to the B2 sub-zones relative to the parent rock, but has only slightly lower enrichment in the B2 and A zones (Fig. 4). Scandium concentrations increase up-section (Fig. 4) suggesting sorting effect (Fedo *et al.*, 1996). Th/Sc ratios show a similar pattern of vertical variation to Al_2O_3/TiO_2 in this section (Fig. 6). The Th/Sc ratios level out in the A zone at values ranging from 1.0 to 1.5, which are close to the composition of average post-Archean shale (Th/Sc=1.0, Taylor and McLennan, 1985; Condie, 1993).

REE patterns

Rare earth elements (REE) display valuable information on provenance, as they are mostly immobile during sedimentary processes and in weathering profiles (Taylor and McLennan, 1985; Price *et al.*, 1991; Condie, 1993; McLennan *et al.*, 1993; Nesbitt and Markovics, 1997). Source rock compositions are often estimated using REE indices such as REE

patterns, Eu anomalies (Eu/Eu*), and La/Yb ratios (Taylor and McLennan, 1985, McLennan *et al.*, 1993; Condie, 1993; Fedo *et al.*, 1996). Nesbitt and Markovics (1997) suggested that Nd/Sm ratios vary least during weathering processes, and it is well established that Nd-Sm model ages from sediments are not affected by chemical weathering.

Parent rock (granodiorite) normalized REE patterns for five samples show remarkably flat patterns (Fig. 7), indicating that no significant fractionation has occurred within the REE during soil formation. In detail, black soil samples (no. 11 and 14, 98.1 and 89.4 ppm respectively) show relative enrichment in $\sum$REE compared to parent rock (no. 1, 80.2 ppm). Lanthanum is slightly enriched relative to that of Ce in the soils relative to the parent in all except the *masa* sand (no. 5). Chondrite-normalized REE patterns (Taylor and McLennan, 1985, Condie, 1993) show mutually similar patterns with little variation in La content and the middle to heavy REE (Fig. 8). They, however, show significant light REE enrichment relative to middle and heavy REE, relatively large negative Eu anomalies [Eu/Eu*=0.5-0.6, excluding one sample (no. 14)], and nearly horizontal patterns for the middle to heavy REE concentrations (Fig. 8). The Eu anomalies show no systematic stratigraphic change within the Minari profile (Fig. 6), despite the change in CIA from the C1 to A zones. Chondrite-normalized Nd/Sm (Nd_N/Sm_N) and La/Yb values (La_N/Yb_N) also show little variation up-section, ranging from 1.45 to 2.17 and 6.0 to 8.5, respectively. Compared to the stratigraphic variation of Th/Sc, the REE indices in the Minari section are significantly less influenced by weathering and sorting effects.
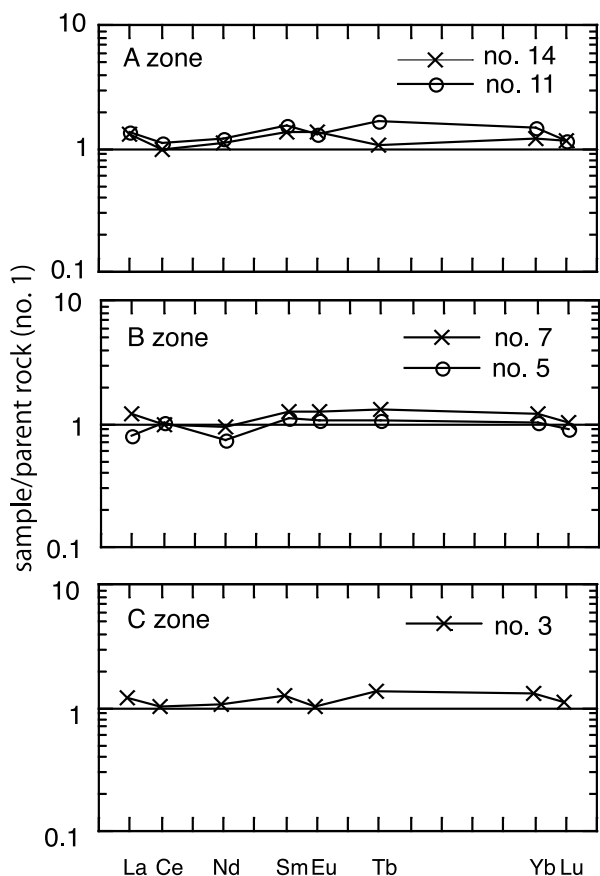
Fig. 7. REE patterns for samples in the Minari section normalized against parent rock (granodiorite) composition, San'in district of Southwest Japan.
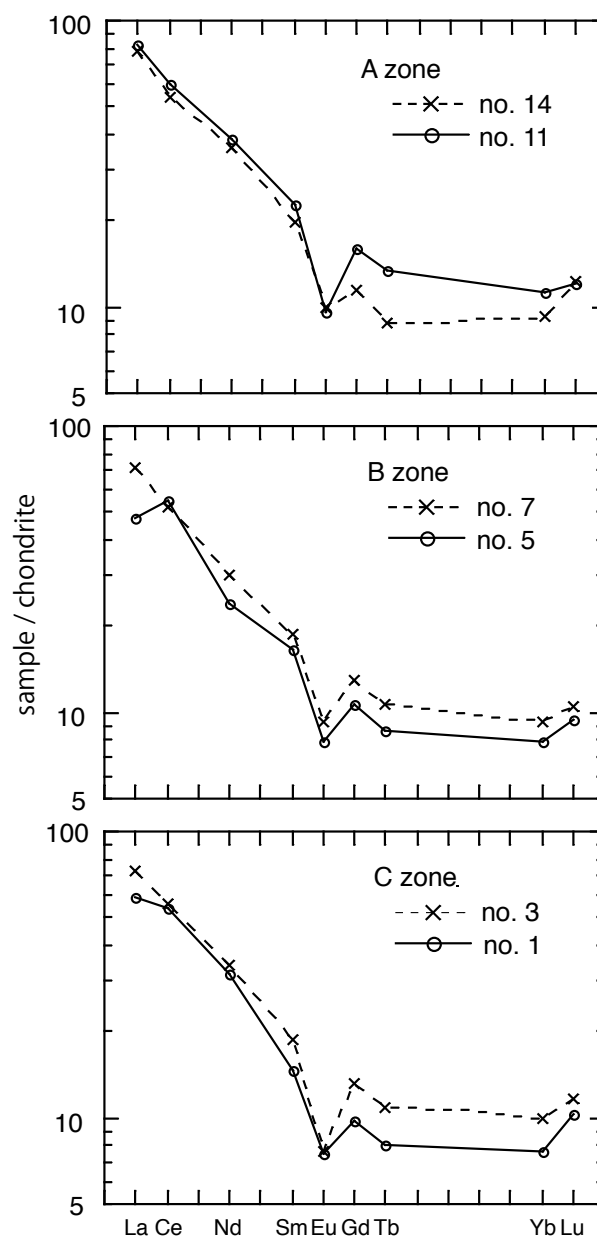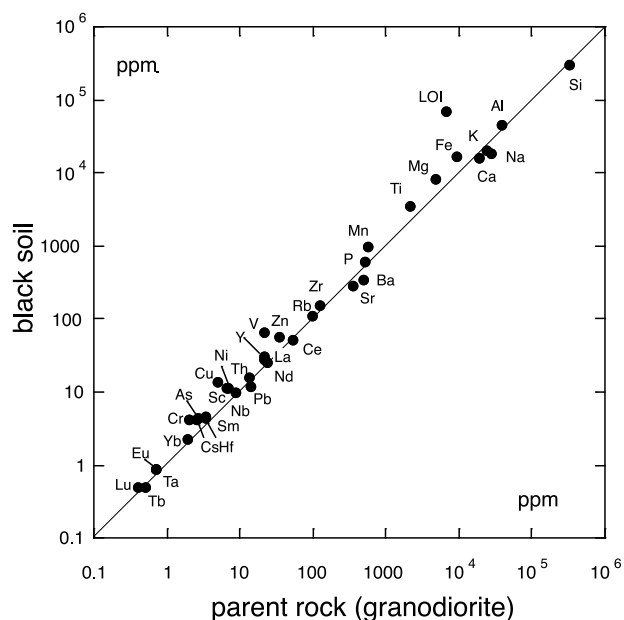

Fig. 9. Comparison of geochemical compositions between the C zone (parent rock of the fresh granodiorite, no. 1) and the A zone (black soil, no. 14) from the Minari section, San'in district of Southwest Japan. Cr concentrations were not detected in either sample (nos. 1 and 14). Cr data for these zones are those of samples no. 3 and no. 13, respectively.

Fig. 8. Chondrite-normalized REE patterns for selected samples from the Minari section, San'in district of Southwest Japan.

Conclusions

The formation of black soils from granitoids in the San'in district has resulted in compositional variation. This variation is shown by enrichment in Fe_2O_3*, TiO_2 and Sc in black soils relative to the concentration of the parent granodiorites, and depletion in Na_2O, CaO, Ba and Sr (Fig. 9). Concentrations of Zr, Hf, Th, Ce, Nb, Ta Pb and Rb, however, remain similar to those of the parents (Figs. 3, 4). CIA ratios range from 52 in slightly weathered granodiorite to 68 in the most weathered soil at Yokota area, still somewhat less than those typical of average shales, and Miocene sedimentary rocks in the San'in district. REE patterns and Eu/Eu*, Nd_N/Sm_N and La_N/Yb_N parameters mostly reflect source material

composition (Fig. 6), as previously indicated by Taylor and McLennan (1985), Cullers *et al.* (1988), McLennan *et al.* (1993), and others. The REE, however, have limitations in the number of analyses, availability may be restricted due to the sophisticated analytical methods required (such as INAA and ICP-MS). Therefore, ratios determinable by XRF, such as Th/Sc, offer advantages of analytical convenience over the REE.

Acknowledgements

References

Abbot, I. and Parker, C. A., 1981, Interactions between earthworms and their soil environment. *Soil Biol. Biochem.*, **13**, 191-197.

Bowen, H. J. M., 1979, Environmental Chemistry of the Elements. Academic Press Inc., London. 367p.

Condie K. C., 1993, Chemical composition and evolution of the upper continental crust: Contrasting results from surface samples and shales. *Chem. Geol.*, **104**, 1-37.

Cullers, R. L., 1994, The chemical signature of source rocks in size fractions of Holocene stream sediments derived from metamorphic rocks in the Wet Mountain regions, Colorado, U.S.A. *Chem. Geol.*, **113**, 327-343.

Cullers, R. L., Basu, A. and Suttner, L. J., 1988, Geochemical signature of provenance in sand-size material in soils and stream sediments near the Tobacco Root batholith, Montana, USA. *Chem. Geol.*, **70**, 335-348.

Cullers, R. L., Chaudhuri, S., Kilbane, N. and Koch, R., 1978, Rare-earths in size fractions and sedimentary rocks of Pennsylvanian-Permian age from the mid-continent of the U.S.A. *Geochim. Cosmochim. Acta,* **43**, 1285-1301.

Editorial Board of Geological Map of Shimane Prefecture, 1997, Geological map of Shimane Prefecture (1:200,000).

Fedo, C. M., Nesbitt, H. W. and Young, G. N., 1995, Unraveling the effects of potassium metasomatism in sedimentary rocks and paleosols, with implications for paleoweathering conditions and provenance. *Geology*, **23**, 921-924.

Fedo. C. M., Kenneth A. E. and Krogstad, E., 1996, Geochemistry of shales from the Archean (~3.0 Ga) Buhwa Greenstone Belts, Zimbabwe: Implications for provenance and source-area weathering. *Geochim. Cosmochim. Acta*, **60**, 1751-1763.

Fyfe, W. S., 1989, Soil and global change. Episodes, **12**, 249-254.

Garcia, D., Fonteiller, S. M. and Moutte, J., 1994, Sedimentary fractionations between Al, Ti, and Zr and genesis of strongly peraluminous granites. *Jour. Geol.*, **102**, 411-422.

Ishiga, H. and Dozen, K., 1997, Geochemical indication of provenance change related to Miocene opening of Japan Sea. *Marine Geology*, **144**, 211-228.

Ishihara, S., 1977, The magnetite-series and ilmenite-series granitic rocks. *Mining Geology*, **27**, 293-305.

Kano, K., Yamauchi, S., Takayasu, K., Matsuura, H. and Bunno, M., 1994, Geology of the Matsue district. With geological Sheet Map at 1:50,000, Geol. Surv. Japan, 126 p.

Kimura, J. and Yamada, Y., 1996, Evaluation of major and trace element XRF analyses using a flux to sample ratio of two to one glass beads. *Jour.* *Min. Petrol. Econ. Geol.*, **91**, 62-72.

McLennan, S.M., Hemming, S., MacDaniel, D. K. and Hanson, G. N., 1993, Geochemical approaches to sedimentation, provenance and tectonics. *Geol. Soc. Am. Spec. Paper*, **284**, 21-40.

Musashino, M., 1990, The Panthalassa- a cerium-rich Atlantic-type ocean: sedimentary environments of the Tamba Group, Southwest Japan. *Tectonophysics*, **181**, 165-177.

Nesbitt, H. W. and Markovics, G., 1997, Weathering of granodiorite crust, long-term storage of elements in weathering profiles, and petrogenesis of siliciclastic sediments. *Geochim. Cosmochim. Acta*, **61**, 1653-1670.

Nesbitt, H. W. and Young, G. M., 1982, Early Proterozoic climates and plate motions inferred from major element chemistry of lutites. *Nature*, **299**, 715-717.

Nesbitt, H. W. and Young, G. M., 1984, Prediction of some weathering trends of plutonic and volcanic rocks based upon thermodynamic and kinetic considerations. *Geochim. Cosmochim. Acta*, **48**, 1523-1534.

Nesbitt, H. W. and Young, G. M., 1989, Formation and diagenesis of weathering profiles. *Jour. Geol.*, **97**, 129-147.

Nesbitt, H. W., Young, G. M., McLennan, S. M. and Keays, R. R., 1996, Effects of chemical weathering and sorting on petrogenesis of siliciclastic sediments, with implications for provenance studies. *Jour. Geol.*, **104**, 525-542.

Nesbitt H. W., Fedo C. M. and Young G. M., 1997, Quartz and feldspar stability, steady and non-steady-state weathering, and petrogenesis of siliciclastic sands and muds. *Jour. Geol.*, **105**, 173-191.

Norrish, H. W. and Hutton, J. T., 1969, An accurate X-ray spectrographic method for the analysis of a wide range of geologic samples. *Geochim. Cosmochim. Acta*, **33**, 431-453.

Ortiz, E. and Roser, B. P., 2006, Geochemistry of stream sediments from the Hino River, SW Japan: source rock signatures, downstream compositional variations, and influence of sorting and weathering. *Earth Science (Chikyu Kagaku)*, **60**, 131-146).

Potts, P. J., Tindle A. G. and Webb P. C., 1992, Geochemical reference material compositions. Whittles Publishing, pp. 313.

Price, R. C., Gray, C. M., Wilson, R. E., Frey, F. A. and Taylor, S. R., 1991, The effects of weathering on rare-earth elements, Y and Ba abundances in Tertiary basalts from southeastern Australia. *Chem. Geol.*, **93**, 245-265.

Rainbird, R. H., Nesbitt, H. W. and Donaldson, J. A., 1990, Formation and diagenesis of a Sub-Huronian saprolith: comparison with a modern weathering profile. Jour. Geol., **98**, 801-822.

Roser, B. P., Cooper R. A. and Tulloch A. J., 1996, Reconnaissance sandstone geochemistry, provenance, and tectonic setting of the lower Paleozoic terranes of West Coast and Nelson, New Zealand. *New Zealand Jour. Geol. Geophys.*, **39**, 1-16.

Roser, B. P. and Korsch, R. J., 1986, Determination of tectonic setting of sandstones mudstones suites using SiO_2 content and K_2O/Na_2O ratio. *Jour. Geol.*, **94**, 635-650.

Roser, B. P. and Korsch, R. J., 1999: Geochemical characterization, evolution and source of a Mesozoic accretionary wedge: the Torlesse terrane, New Zealand. *Geol. Mag.*, **136**, 493-512.

Taylor, S. R. and McLennan, S. M., 1985, The Continental Crust: its composition and evolution. Blackwell, Oxford, 312 pp.

Tokuoka, T., Onishi, Y., Takayasu, K. and Mitsunashi, T., 1990, Natural history and environmental changes of Lakes Nakaumi and Shinji. *Mem. Geol. Soc. Japan*, **36**, 15-34.

Wronkiewicz, D. J. and Condie K. C., 1987, Geochemistry of Archean shales from the Witwatersrand Supergroup, South Africa: Source-area weathering and provenance. *Geochim. Cosmochim. Acta*, **51**, 2401-2416.

Yamanoi, T., 1996, Geological investigation on the origin of the black soil distributed in Japan. *Jour. Geol. Soc. Japan*, **102**, 526-544.

（要　旨）

石賀裕明・道前香緒里・山﨑静子, 2013 花コウ岩質岩石の風化と黒色土壌の形成についての地球化学的
意義－西南日本の山陰地域の例. 島根大学地球資源環境学領域研究報告, 32, 1-11.

　　　花コウ岩質岩石の化学的風化と黒色土壌形成時における土壌形成に関連する分級作用について西
南日本の山陰地域の横田において検討した. 検討した三成セクションは 3 帯（上位より A, B, C 帯）
に区分される. C 帯は新鮮な花コウ岩類（C1）と初生の組織を持つ風化した花コウ岩（C2）であ
る. B 帯は風化した花コウ岩類で砂粒度の基質に角レキを伴うもの（B1）と細粒化が進み酸化鉄が
部分的にしみたもの（B2）である. A 帯は黒色土壌で有機物に富み, 3 帯の中では LOI（強熱減量）
は 6-7 wt% と最も高い.

　　　LOI と CIA（化学的風化指数）はこの土壌断面で徐々に増加し, 風化は地表へ向けて漸移的に増
加する. SiO_2 は C 帯ではあまり変化しないが, Fe_2O_3, K_2O を除くその他の主元素は上位に向けて減
少する.

　　　A-CN-K ダイヤグラムでは C, B 帯の試料は K に富む傾向を示し, A 帯の試料は最も高い CIA 値
を持つ. 横田から採取されたその他の黒色土壌はこのダイヤグラムの頂点 A に向かってプロットさ
れ, このことは A 帯の土壌よりも強い風化もしくは分級作用を受けたと言える.

　　　Ni と Zn は垂直変化ではやや増加する. Pb, Rb についてはより変化は少ない. 一方, Zr, Hf, Th, Ce,
Nb と Ta については変化が少ない. このような元素の移動についてみると, Ti/Zr, Zr/Y, Th/Sc 比な
どは源岩組成を反映していると言える. また, REE パターンや Eu/Eu*, La_N/Yb_N, Nd_NSm_N は層序的
に最も少ない変化を示し, このことから REE は黒色土壌形成においても相対的に移動しないことを
反映する.